

# MORPHOLOGY AND OPTICAL PROPERTIES OF TETRAGONAL Ge NANOCCLUSERS GROWN ON CHEMICALLY OXIDIZED Si(100) SURFACES

V.S. LYSENKO,<sup>1</sup> S.V. KONDRATENKO,<sup>2</sup> YU.N. KOZYREV,<sup>3</sup>  
M.YU. RUBEZHANSKA,<sup>3</sup> V.P. KLADKO,<sup>1</sup> YU.V. GOMENIUK,<sup>1</sup>  
O.Y. GUDYMENKO,<sup>1</sup> YE.YE. MELNICHUK,<sup>2</sup> G. GRENET,<sup>4</sup>  
N.B. BLANCHARD<sup>5</sup>

<sup>1</sup>V.E. Lashkaryov Institute of Semiconductor Physics, Nat. Acad. of Sci. of Ukraine  
(41, Prosp. Nauky, Kyiv 03028, Ukraine)

<sup>2</sup>Taras Shevchenko National University of Kyiv  
(64, Volodymyrs'ka Str., Kyiv 01601, Ukraine; e-mail: kozyrev@iop.kiev.ua)

<sup>3</sup>O.O. Chuiko Institute of Surface Chemistry, Nat. Acad. of Sci. of Ukraine  
(17, General Naumov Str., Kyiv 03164, Ukraine)

<sup>4</sup>Université de Lyon, Institut des Nanotechnologies de Lyon INL-UMR5270  
(CNRS, Ecole Centrale de Lyon, Ecully, FR-69134, France)

<sup>5</sup>Laboratoire de Physique de la Matière Condensée et Nanostructures Université Lyon 1  
(CNRS, UMR 5586 Domaine Scientifique de la Doua F-69622 Villeurbanne cedex; France)

PACS 73.63.-b; 79.60.Jv;  
85.45.Db  
©2012

Germanium (Ge) nanoclusters are grown by the molecular-beam epitaxy technique on a chemically oxidized Si(100) surface at 700 °C. X-ray diffraction and photocurrent spectroscopy demonstrate that the nanoclusters have the local structure of body-centered-tetragonal Ge, which exhibits an optical adsorption edge at 0.48 eV at 50 K. Deposition of silicon on the surface with Ge nanoclusters leads to the surface reconstruction and the formation of a polycrystalline diamond-like Si coverage, while the nanoclusters core becomes a tetragonal SiGe alloy. The intrinsic absorption edge is shifted to 0.73 eV due to the Si–Ge intermixing. Possible mechanisms for nanoclusters growth are discussed.

Applications of Ge on SiO<sub>2</sub> structures include CMOS transistors [3] and nanocrystal nonvolatile memory [4, 5].

The technique of Ge nanoisland growth on Si(100) covered with ultrathin SiO<sub>2</sub> layers is widely accepted now [6]. This technique enables increasing the nanoisland density up to 10<sup>12</sup>–10<sup>13</sup> cm<sup>-2</sup> due to the thermal decomposition of the ultrathin oxide layer and the formation of “defects” at the surface, which are nucleation centers for both epitaxial and nonepitaxial Ge nanoislands with high aspect ratio varying between 0.2 and 0.6 [7, 8]. Moreover, Ge nanoislands grown by this method do not contain an underlying germanium wetting layer as for the Stranski–Krastanow mode.

Nonepitaxial Ge nanoislands which are separated from a substrate attract special interest due to the spatial separation of electron-hole pairs leading to a reduction of the recombination rate [9]. NI's growth at the surface with an ultrathin silicon oxide layer is mainly determined by the dynamics of changes of the SiO<sub>x</sub> film structure and physical properties during the Ge deposition and is principally possible at temperatures below ~ 400 °C, when the formation of voids in ultrathin SiO<sub>2</sub> films is suppressed [10]. Epitaxy at such low temperatures puts some limitations on the crystallinity and the structural perfection of the obtained nanoclusters. Increasing the growth temperature up to 430 °C allows one to grow epitaxial crystalline NI's on silicon, while silicon oxide will disappear due to the thermal decomposition effect [7]. Possibility for the high-temperature growth of crys-

## 1. Introduction

Germanium nanoclusters grown on/in silicon or silicon dioxide have been successfully applied in new nanoelectronic, optoelectronic, and memory devices due to the quantum confinement effect and the possibility of integration within the Si-based technology [1, 2]. Heterostructures with epitaxial Ge nanoclusters isolated from the Si substrate by an ultrathin silicon oxide layer would be practically promising due to their nanoscale size, tunability, and high density. The interest in the optoelectronic and solar cells application stems from the observation of infrared photoluminescence and photoconductivity caused by optical transitions through confined states of Ge nanoislands (NI). Other important ap-

talline Ge NI's on the top of silicon oxide has not been studied in detail. The question under study is which type of structure of Ge nanoclusters will arise after high temperature growth in the presence of a tetragonal silicon oxide film giving poor relationship with underlying Si (100).

In this paper, the technique is suggested for the high-temperature growth of crystalline Ge nanoclusters on a chemically oxidized Si surface with the initial 2-nm-thick oxide layer, which allows creating the dense arrays of nanoclusters with the tetragonal structure. The main features of the proposed growth mode is the preliminary high-vacuum annealing of a silicon dioxide film at 800 °C leading to the phase separation [11]. For the first time, the Ge nanoclusters with the body-centered-tetragonal (bct) crystal lattice, which are the small band gap material with the absorption edge around 0.48 eV, were obtained.

## 2. Experimental Details

The Ge nanocluster structures were grown using the molecular beam epitaxy (MBE) technique on boron-doped ( $N_a \sim 10^{17} \text{ cm}^{-3}$ ) *p*-Si(100) substrates with the resistivity of 7.5  $\Omega\cdot\text{cm}$ . A pre-epitaxial chemical oxidation of silicon resulted in the formation of a 2-nm-thick SiO<sub>2</sub> layer on the substrate. The surface modifications were monitored *in situ* using the reflection high-energy electron diffraction (RHEED) technique. The Debye rings in the electron diffraction image showed the presence of an amorphous silicon oxide layer. Before the deposition of Ge, the oxidized silicon surface was annealed in vacuum ( $\sim 10^{-10}$  Pa) at a temperature of about 800 °C for an hour. The diffraction pattern has changed, and the appearance of clear and bright Kikuchi lines allows us to conclude, taking the film thickness and the annealing temperature into account, that the phase separation and crystallization in the oxide layer has occurred [11]. As a result, the film can be considered as a silicon suboxide SiO<sub>*x*</sub> ( $0 < x < 2$ ) having silicon-rich regions. Then the substrate temperature was lowered to 700–730 °C, and the deposition of germanium was performed, leading to the formation of Ge nanoclusters on the top of the SiO<sub>*x*</sub> layer (structure A).

After the deposition of Ge nanoclusters, half of the wafer was covered by a mask, and the system was exposed to a weak flow ( $2\text{--}3 \times 10^{14} \text{ cm}^2/\text{s}$ ) of Si atoms. As a result, Si/Ge nanoclusters were formed on the uncovered part of the wafer due to the additional deposition of silicon with a nominal thickness of around 8 monolayers (structure B). Finally, a part of the wafer

with as-grown Ge nanoclusters was covered by a 25-nm-thick Si layer (structure C). During the deposition of silicon on Ge nanoclusters, the transformation of the 1×1 RHEED pattern to a high-resolution 2×1 one was observed, which is typical of the growth of the flat surface of Si(100).

Different experimental techniques were employed to characterize the size of nanoclusters. Size distribution and surface densities of the nanoclusters were controlled, by using atomic force microscopy (AFM) with the scanning of the uncovered structures grown under the same conditions. AFM measurements were performed with an NT-MDT Ntegra microscope in the semicontact tapping mode using Si cantilevers with a tip apex radius of  $\sim 10$  nm. High resolution transmission electron microscopy (HRTEM) observations of the local structure of islands and the oxide film were performed on a Gemini microscope operating at 200 kV.

X-ray diffractograms for the phase analysis were registered with an X'Pert PRO MRD diffractometer in the reflected beam (Cu  $K_\alpha$  radiation,  $\lambda = 1.5418 \text{ \AA}$ ) in the range of angles  $2\theta = 20^\circ\text{--}70^\circ$  with the scanning step of  $0.02^\circ$  and the acquisition time 5–30 s for each point.

Ohmic Au–Si contacts of rectangular shape and dimensions of 4×1 mm were welded into epitaxial layers at 370 °C for lateral photoconductivity measurements. The distance between contacts on the sample surface was 5 mm. Current-voltage characteristics of the structures studied were found to be linear in the range from –10 V to +10 V at temperatures between 50 and 290 K. Lateral photoconductivity spectra were measured at excitation energies ranging from 0.48 to 1.7 eV under illumination with a 250-W halogen lamp. The corresponding direct photocurrent signal was registered by a standard amplification technique. Spectral dependences were normalized to the constant number of exciting quanta using a nonselective pyroelectric detector.

## 3. Results

### 3.1. Surface morphology of Ge nanoislands

The atomic force microscopy image in Fig. 1,*a* shows that the deposition of germanium onto the SiO<sub>*x*</sub> film at 700 °C results in the formation of nanoclusters with the hemispherical top surface and the surface density of  $\sim 3 \times 10^{11} \text{ cm}^{-2}$ . The base diameter distribution of Ge nanoclusters is approximated by a Gaussian function with the maximum at 16 nm and a full width at half maximum of 6 nm. The mean height was about 10 nm. The surface of the structure with Ge islands covered by

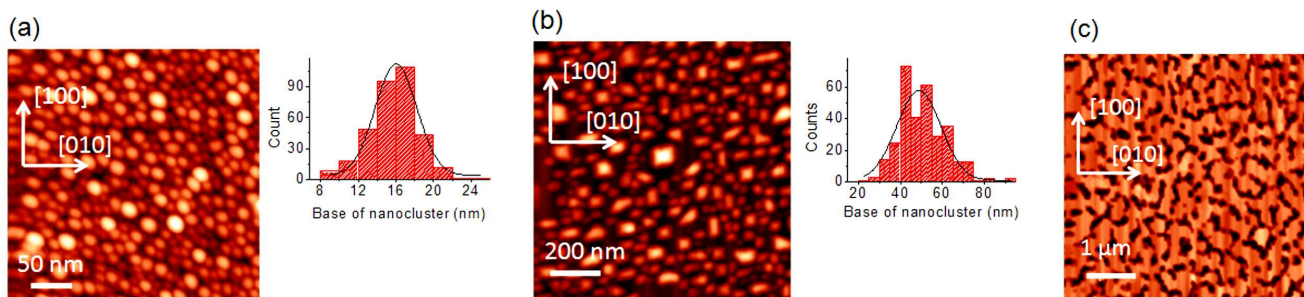


Fig. 1. *a*) AFM image of the surface with Ge nanoislands, grown on the surface of a  $\text{SiO}_x$  film and distributions of nanoclusters over base diameters (structure A); *b*) the same for the surface modified by the deposition of Si on the structure with Ge nanoislands (structure B); *c*) AFM image of the surface of structure C with Ge nanoclusters covered by a 25-nm-thick Si layer

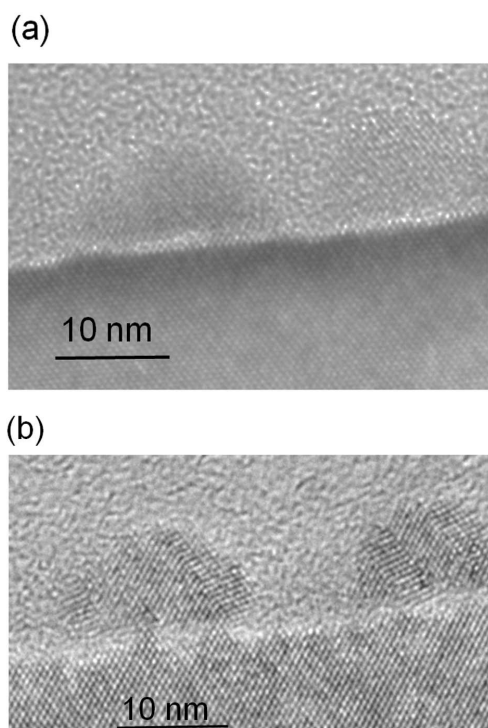


Fig. 2. HRTEM images of Ge nanoclusters grown on silicon oxide

a Si layer is shown in Fig. 3, *c*. The surface of capping Si for structure C contains voids with depth 25 nm.

A typical HRTEM image of Ge nanoclusters grown on silicon oxide is plotted in Fig. 2. We can see that the aspect ratio (height/base) of 0.6 for Ge islands on silicon oxide is much larger than typical values 0.1–0.15 for Stranski–Krastanow islands [12]. The Ge nanoclusters have a crystalline structure, but its quality is strongly affected by twin boundaries. However, the most of Ge nanocrystals demonstrate perfect crystallization without any defects. Observation of perfect crystal planes for the

Si substrate shows the high quality of the HRTEM images.

After the deposition of Si atoms onto the surface with Ge nanoclusters, the surface morphology changes (Fig. 1, *b*): the mean size of formed Si/Ge nanoclusters increases, and their surface density decreases to  $\sim 10^{10}$  / $\text{cm}^2$ , i.e. becomes by a factor of 30 less as compared to the Ge nanocluster density for the as-deposited structure. The base diameter distribution of Si/Ge nanoclusters is approximated by a Gaussian function with the maximum at 50 nm and an essentially larger full width at half a maximum of 24 nm. The base of the formed Si/Ge nanoclusters is no longer circular after the surface reconstruction. In the bases of nanoclusters, polygons are observed. The average distance between clusters is about 15 nm.

### 3.2. X-ray diffractometry

Grazing incidence X-ray diffractograms of the studied samples are presented in Fig. 3 (curves 1–3). The diffractograms were registered at different incident angles of the X-ray beam (XB) in order to detect the phases from thin layers. In diffractograms for all the samples, strong reflexes 111 and 200 related to Au (contact material) at various incident angles are observed. In the diffractogram of the sample with Ge nanoislands grown on the chemically oxidized Si(100) surface (curve 1), a weak peak at the angle  $2\theta = 24.78^\circ$  was observed at different incident angles of XB. This peak is also present in the diffraction spectra of the structure with 8 monolayers (MLs) of Si deposited onto the surface with Ge nanoclusters. It can be attributed to reflex 111 of the tetragonal modification of Ge (ICDD, PDF-2, 01-072-1089 (Tetragonal **II-Ge**:  $a = b = 5.93 \text{ \AA}$ ,  $c = 6.98 \text{ \AA}$ )). In diffraction patterns of the structure with Si/Ge nanoclusters at a sliding angle of XB, the peak is observed

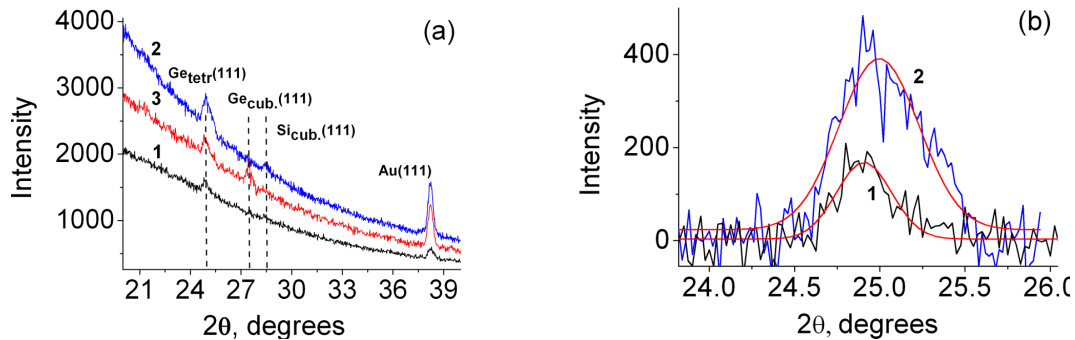


Fig. 3. *a*) X-ray diffraction spectra for samples recorded at the incident angle  $\omega = 0.5^\circ$ . 1 – as-grown sample with Ge nanoclusters grown on chemically oxidized Si(100); 2 – with 8 MLs of Si; 3 – structure with Ge nanoclusters covered by a 25-nm-thick Si layer. *b*) Peaks subtracted from spectra for the as-grown sample with Ge nanoclusters and the sample with 8 MLs of Si

at the Bragg angle  $2\theta = 28.587^\circ$ , close to the diffraction angle for the cubic phase of silicon (reflex 111). This peak can be attributed to the solid solution  $\text{Si}_{1-x}\text{Ge}_x$  ( $x \sim 0.7$ ), which is formed due to the intermixing of Si and Ge atoms during the silicon epitaxy onto the surface of Ge nanoclusters. In this case, the average germanium content  $x = 0.7$  was estimated using the Vegard's relation [13]:

$$a_{\text{SiGe}} = (1 - x)a_{\text{Si}} + xa_{\text{Ge}}. \quad (1)$$

Here,  $a_{\text{SiGe}}$  is the measured value of the lattice parameter (from the Bragg angle position of peak 111),  $a_{\text{Si}}$  and  $a_{\text{Ge}}$  are the tabulated values of lattice parameters for silicon and germanium, respectively.

In diffraction spectra of the sample with the 25-nm Si layer deposited onto the surface with Ge nanoclusters, the intensity of reflex 111 for the tetragonal Ge phase decreases, and the reflex appears at  $27.5^\circ$ , close to the diffraction angle from the cubic phase of germanium 111  $\text{Ge}_{\text{cub}}$  (curve 3). The peak at  $2\theta = 28.587^\circ$ , which was observed for the structure with Si/Ge nanoclusters, is not present (Fig. 3, curve 2).

Since the reflexes are present in the diffraction spectra for different reflections from clusters and silicon layers both in sliding and in symmetric geometries, the conclusion can be drawn that the material of clusters and the silicon layer have a polycrystalline structure. However, we could detect and analyze experimentally only the strong reflex 111.

The average size of Ge nanoclusters can be approximately determined from the Scherrer equation:  $L = \lambda / \Delta\theta \cos\theta$ , where  $\Delta\theta$  is the line broadening at half the maximum intensity,  $\lambda$  is the X-ray wavelength, and  $\theta$  is the Bragg angle. The derived values of the sizes of nanoislands varied from 18 nm for the as-grown structures to 40 nm for the structure covered by silicon, which

is in good agreement with AFM data. The dispersion of dimensions  $\sigma$  is large and was found to be about 7.5 nm. The Scherrer equation for a single reflex gives estimation of the object size in the direction normal to the reflecting planes (in our case – in direction 111).

### 3.3. Photocurrent spectra

To study experimentally the optical absorption spectra of the structures with nanoclusters, we used the spectroscopy of lateral photoconductivity [14, 15]. This technique allows studying the spectral features of nano-sized objects, whose contribution to the total light absorption is weak due to small sizes of investigated structures. Spectral dependences of photoconductivity were measured in a wide temperature range from 50 to 290 K. The contribution of nonequilibrium carriers, excited in nanoclusters, increases at lower temperatures. Figure 4 shows the lateral photoconductivity spectra at 50 K for Ge-SiO<sub>x</sub>-Si heterostructures with Ge nanoclusters at the SiO<sub>x</sub> surface (curve 1), for the heterostructure with Si/Ge nanoclusters (curve 2), and for the structure with Ge nanoclusters covered by a 25-nm thick-Si layer (curve 3).

In the structure with Ge nanoclusters, the photoconductivity edge was found at the quantum energy  $h\nu > 0.48$  eV. The deposition of Si onto the surface with Ge nanoclusters leads to a shift of photoconductivity (absorption) spectra toward higher energies of quanta (Fig. 3, curve 2). The long-wavelength edge of photoconductivity spectra was observed at around 0.73 eV. The subsequent deposition of the 25-nm-thick Si layer onto the surface with Si/Ge nanoislands did not cause a further modification of the spectra (Fig. 4, curve 3) However, in the heterostructure with Ge nanoislands covered

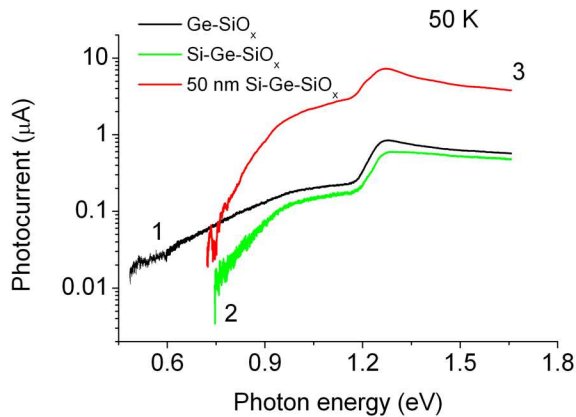


Fig. 4. Lateral photoconductivity spectra at 50 K for heterostructures with Ge nanoclusters at the  $\text{SiO}_x$  surface (curve 1), for the structure with Ge nanoclusters modified by Si deposition (curve 2) and for the structure with a 25-nm-thick Si layer deposited on the top of Ge nanoclusters (curve 3)

by the 25-nm-thick Si layer, the photoresponse and the dark conductivity were an order of magnitude higher.

#### 4. Discussion

The use of a chemically oxidized Si surface with the initial 2-nm-thick  $\text{SiO}_2$  film allows the formation of crystalline Ge nanoclusters, which are separated from the substrate by a thin oxide layer, at high ( $\sim 700$  °C) temperatures. One of the key differences of the proposed technique for the formation of Ge nanoclusters is a preliminary modification of the chemically oxidized Si(100) surface. During the high-vacuum annealing of the  $\text{SiO}_2$  film at 800 °C for an hour, the thermal decomposition of the silicon dioxide film takes place according to the reaction



As a result, the nonstoichiometric  $\text{SiO}_x$  ( $x \leq 2$ ) layer is formed containing nonbridging oxygen hole centers and first oxygen-deficiency centers ( $E'$  centers). Two neighboring  $E'$  centers can be transformed into the neutral oxygen vacancy, in which two incomplete tetrahedra are linked by the Si–Si bond [16]. The Si–Si bonds on the top of the oxide film are nucleation centers for the Ge nanocluster formation. During the deposition of the first germanium monolayer onto silicon oxide, the absorption layer is formed, which, starting just from the second monolayer, is transformed into nanoclusters that nucleate randomly on the top of chemical  $\text{SiO}_2$ . Such a type of the surface reconstruction is energetically favorable in

the case where the direct contact with the Si(100) substrate is absent, i.e., when the oxide layer is still present [17].

AFM image confirms a poor relationship with the silicon substrate. We can see the two types of Ge nanoclusters grown on the oxide film. The smallest clusters shown in Fig. 1, *a* have a circle base. The large islands are oblong in shape, having base sides oriented randomly with respect to substrate directions, which are resulted from the coalescence of many smaller islands. The presented images show also examples of two Ge nanoclusters that have just begun the coalescence. It is significant to note that the boundaries between merged clusters have different in-plane tilts with respect to [100] and [010] directions of the Si substrate. We can suppose that Ge nanoclusters have a poor epitaxial relationship with the Si(100) substrate, i.e., are tilt-misoriented to the underlying Si substrate. The HRTEM image shows the presence of defect-free crystalline Ge nanoclusters, which are separated from Si(100) by a silicon oxide film with a thickness of 1 nm (Fig. 2, *a*). A reduction of the oxide thickness from the initial value of 2 nm to 1 nm is the evidence of the pre-growth thermal destruction of silicon dioxide according reaction (3). Crystalline clusters in silicon oxide beneath of Ge nanoclusters start to nucleate during the high-vacuum annealing of the oxide film at 800 °C, while  $\text{SiO}_x$  film separates into more stable  $\text{SiO}_2$  and Si clusters. We can also exclude that the formation of crystalline clusters in silicon oxide continues during the Ge growth. The presence of similar localized inclusions in the ultrathin silicon oxide film that exhibit the single crystalline character has been previously reported in [18, 19]. The width of these clusters is 2–3 nm and the surface density is  $10^{11} \text{ cm}^{-2}$ , which agrees with the observed density of Ge nanoclusters.

X-ray diffraction spectra show a tetragonal crystalline structure of Ge nanoclusters grown on oxide films, which points to a more complex mechanism of nanoclusters formation, than the nucleation on silicon voids described in [18, 19]. The crystalline voids shown in Fig. 2, *b* may arise under nanoclusters during the formation of Ge nanoclusters. They are centers of defect generation due to the effect of the Si cubic lattice on a crystal structure of Ge tetragonal nanoclusters, which were nucleated randomly and had no relationship to the substrate initially. Twin boundaries are observed in some part of Ge nanoclusters having direct contacts to the substrate through crystalline regions (Fig. 2, *b*). The high-density twin defects have also been observed in Ge films created from the nucleation and the coalescence of Ge islands within small crystalline openings in the  $\text{SiO}_2$  template in twin

relationship to the silicon substrate [20]. The twinning of the (111) planes is also observed for Ge nanoclusters embedded in SiO<sub>2</sub>, while the distance from islands and the Si(100) substrate is less than 2 nm [11].

In spite of the connection to the substrate through crystalline regions in oxide, the usual diamond-like crystal structure of Ge appears to be completely absent in nanoclusters grown on the oxide film. When the initial stage of nanoclusters growth on the oxide layer takes place, the epitaxial relationship with the Si(100) substrate is poor, and Ge nanoclusters with tetragonal structure are created, because the type of their crystal lattice is determined mainly by a local structure of the SiO<sub>x</sub> film near the sites of the generation of nucleation centers. In the process of Ge epitaxy, the Si–O chemical bonds nearest to the cluster nucleation centers are being broken, which leads to the substitution of oxygen atoms by Ge atoms and to the formation of a tetragonal polycrystalline structure. The existence of the body-centered-tetragonal phase (Ge II) is secured by compressive deformations, appearing when Ge adatoms are linked to the nanocluster nucleation centers (Si–Si bonds) due to different lengths of Si–O cristobalite (1.63 Å) and Ge–Ge (2.45 Å) bonds [21, 22]. As described in [21], another of the possible ways for obtaining the body-centered-tetragonal phase of germanium (Ge II) is the heteroepitaxial growth on the (111) surface of a Ge–Sn buffer layer. There are experimental reports of a simple tetragonal structure of Ge nanocrystals [23–25]. In bulk, the tetragonal Ge phase is only obtained from high-pressure experiments. For example, the semiconducting diamond-structure phase (or Ge I) can be transformed to the  $\beta$ -tin structure (or Ge II) at a hydrostatic pressure of approximately 100 kbar [26]. The reason for the long-term tetragonal lattice conservation for Ge nanoclusters is not presently understood.

The stability of the tetragonal phase was also checked by the deposition of Si atoms on Ge nanoclusters. Epitaxy of Si on the surface of the structure with tetragonal Ge nanoclusters leads to an essential modification of the surface topology and morphology. AFM observation, shown in Fig. 1, *b* for sample B, indicate a dramatic decrease of the density of nanoclusters. An irregular shape of nanoclusters is due to the coalescence intensified by the silicon deposition. It can be suggested that, at the initial stages of heteroepitaxy, Si adatoms are selectively linked only to dangling Ge bonds at the surface of nanoclusters. Though the reaction of thermal decomposition of silicon oxide (2) may take place at the oxidized silicon surface between Ge nanoclusters, the new open-

ings of the Si(100) substrate can also be formed despite the presence of a sufficiently thick oxide layer. Because of the lattice mismatch between Ge and Si in the process of nanoisland growth, the elastic energy is accumulated, and the distance between the bases of adjacent nanoclusters reduces. While reaching the critical magnitude of deformation, the total energy of the system can decrease at the expense of a collapse of the spacing between nuclei and due to a reduction of the surface energy. Coalescence of nanoclusters occurs when the sum of the elastic energy generated in the unit area and the grain boundary energy is equal to the energy of two free surfaces of separate crystallites. In this case, the tetragonal structure of Si/Ge nanocrystallites is kept. Their aggregation into nanoclusters is provided by the epitaxy of the linking material – Si. The evidence of the described polycrystallinity is the polygonal base of formed Si/Ge nanoclusters (see Fig. 1, *b*) and a substantial (by a factor of 30) reduction of the surface density of nanoclusters after the surface reconstruction. The smallest clusters have a complicate (polygonal) shape with different orientations of sides. The larger nanoclusters have rectangular base with sides oriented along [100] and [010] directions of underlying Si(100), i.e. have relationship to the substrate due to the decomposition of the oxide layer during the coalescence and the deposition of silicon.

It should be mentioned that, at the used temperatures of nanocluster growth to be about 700 °C, the possibility of the Si penetration into Ge nanoclusters with the formation of Si<sub>1-x</sub>Ge<sub>x</sub> alloy with the tetragonal modification cannot be ruled out. The reflex of the tetragonal germanium phase in the diffraction spectra of the structures with Ge nanoclusters was found at 24.9° (see Fig. 2, *b*). After the Si deposition, the shift of the peak was observed from tetragonal Ge by 0.1° toward greater angles, indicating a reduction of the lattice parameter during the formation of Si<sub>1-x</sub>Ge<sub>x</sub> alloy with the tetragonal lattice. Moreover, the increase of the peak width for Ge nanoclusters can be related to the Si content gradient in nanoclusters.

The appearance of the diffraction peak Si(111) at the Bragg angle  $2\theta = 28.587^\circ$  indicates that the shell of nanoclusters also appears to be crystalline with a cubic unit cell Si (or Si<sub>1-x</sub>Ge<sub>x</sub> alloy with low Ge content). Thus, silicon at the surface of Si/Ge nanoclusters does not continue creating a tetragonal lattice. This effect is evidently explained by the fact that, in the case of the bct Si lattice formation at the surface of Ge nanoclusters, the lattice mismatch would generate tensile stresses in capping Si. The sign of generated deformations makes

the process of creation of cubic Si (or  $\text{Si}_{1-x}\text{Ge}_x$  alloy), instead of its tetragonal modification, more energetically favorable.

After the capping of Ge nanoclusters by the 25-nm Si layer, the SiGe cubic phase is also formed, possibly, due to a reduction of the fraction of the tetragonal phase. The possible reason for this effect is the relaxation of elastic stresses in nanoclusters due to the Si–Ge intermixing. In addition, in the process of Si epitaxy, the destruction of the oxide layer between adjacent Si/Ge nanoclusters may take place, which can lead to the possibility of multiple contacts to the Si(100) substrate, promoting the construction of a cubic lattice. New crystalline voids in oxide films are a source of numerous defects and a crystalline structure disorder of capping Si. The AFM image of sample C shows a discontinuous Si film containing the 25-nm-depth emptiness and confirms the strong influence of defects on its formation. Apparently, the disappearance of the diffraction peak Si(111) at the Bragg angle  $2\theta = 28.587^\circ$  for structure C, in contrast to that observed for structure B, indicates a disordered structure of the Si film.

Measurements of infrared photoconductivity confirmed the above suggestions about the structure of nanoclusters and made it possible to evaluate their electronic spectrum. The contribution of electron-hole pairs photoexcited in Si is observed, when the quanta energy exceed the band gap value. In the spectral range  $h\nu < 1.1$  eV, in which *c*-Si is transparent, the interband indirect transitions take place via the states in the valence and conduction bands of nanoclusters. Nonequilibrium carriers photoexcited in nanoclusters do not contribute into the carrier transport directly. In order to contribute into the lateral current, the nonequilibrium electrons and holes should be spatially separated. As for Ge/Si heterojunctions, the studied systems are referred to II type, where the strong confinement for holes in the region of Ge nanoclusters occurs. In the studied heterostructures, electrons can tunnel through the oxide  $\text{SiO}_x$  film into the near-surface silicon region and make contribution to the conductivity. At the same time, nonequilibrium holes are localized in the valence band of Ge nanoclusters. However, they can affect the potential relief in the near-surface region of the Si substrate, and hence, make an indirect effect on the conductivity. The studies of a.c. and d.c. conductivity will be presented in detail in the next paper.

Thus, the photoconductivity of the structures in the range of Si transparency is unipolar. The intrinsic absorption of light in nanoclusters leads to an increase of

the electron concentration in the Si potential well near the  $\text{SiO}_x$ –Si interface and to an increase of the surface conductance. In this case, the shape of lateral photoconductivity spectra reflects main features of the intrinsic absorption of light in nanoclusters.

Photocurrent spectroscopy and X-ray diffraction demonstrate that the nanoclusters have the local structure of bct Ge, which exhibits the optical adsorption edge at 0.48 eV. Taking the quantum-size effect into account, this is in good agreement with the theoretical calculations of electronic and optical properties of bulk bct Ge and Si, according to which the band gap widths for the mentioned polytypes are 0.38 and 0.86 eV, respectively [21].

The intrinsic absorption edge for nanoclusters with the silicon coverage is shifted to 0.73 eV due to the Si–Ge intermixing, which is confirmed by X-ray diffraction measurements. The observed “blue” shift is due to the formation of tetragonal SiGe nanoclusters, whose band gap width is larger than that of tetragonal Ge. The adsorption of pure Ge nanoclusters was completely absent in structures with deposited silicon. Moreover, the Si–Ge interdiffusion leads to a decrease of the valence band offset. As a consequence, we observed a lower value of photocurrent for structure B as compared with that for structure A due to the enhanced rate of electron-hole recombination through interface states.

It should also be mentioned that, in the formation of a polycrystalline silicon layer, stacking faults are created mainly on the nanocluster boundaries. It was shown experimentally and theoretically that such defects create deep levels in the band gap of silicon. In the spectra of the structures with a polycrystalline diamond-like Si coverage, the component of the photocurrent can be distinguished in the range with the edge at  $\sim 0.8$  eV, which was not observed in the spectra of the structure with Ge nanoclusters. This feature can be explained by transitions via deep levels in polycrystalline Si. It is known that the nanostructured silicon layers grown on a layer of germanium islands on the oxidized silicon surface are characterized by a broad photoluminescence (PL) band with the maximum at around 0.8 eV [27]. The physical reason for the appearance of such PL band is the optical transitions via defect and dislocation levels in Si [28], which leads to the observation of PL bands (D1–D4) at low temperatures with maxima at 0.807, 0.870, 0.935, and 1.0 eV. We cannot rule out that the contribution to the photoconductivity at  $h\nu > 0.8$  eV is due to the optical transitions via the deep defect states of silicon.

## 5. Conclusions

Germanium nanoclusters have been grown by the molecular-beam epitaxy technique on a chemically oxidized Si(100) surface at 700 °C. They appeared to have a high density of about  $3 \times 10^{11} \text{ cm}^{-2}$  and a height of about 10 nm. A possible mechanism for the initial stage of nanocluster growth is associated with the creation of Si–Si bonds during the vacuum annealing of SiO<sub>2</sub>, which act as nucleation centers. X-ray diffraction and photocurrent spectroscopy demonstrate that the nanoclusters have the local structure of body-centered tetragonal Ge, which exhibits an optical absorption edge at 0.48 eV. The usual diamond-like crystal structure of Ge nanoclusters appears to be completely absent due to the isolation from the Si(100) substrate. The further deposition of silicon on the surface with Ge nanoclusters leads to the surface reconstruction and the formation of a polycrystalline diamond-like Si coverage, while the nanoclusters core becomes a tetragonal SiGe alloy. The intrinsic absorption edge for nanoclusters with a silicon coverage is shifted to 0.73 eV due to the Si–Ge intermixing.

The research was supported by the program of fundamental research of the National Academy of Sciences of Ukraine “Nanostructured systems, nanomaterials, nanotechnologies” through the Project No. 9/07 and by the Ministry of Education and Science of Ukraine through Project No. M/34-09.

1. K. Brunner, Rep. Prog. Phys. **65**, 27 (2002).
2. O.G. Schmidt and K. Eberl, Phys. Rev. B **61**, 13721 (2000).
3. G. Masini, L. Colace, and G. Assanto, Mater. Sci. Eng. B **89**, 2 (2002).
4. S. Tiwari, F. Rana, K. Chan, H. Hanafi, C. Wei, and D. Buchanan, IEEE Int. Electron Dev. Meet., 521 (1995).
5. J.H. Wu and P.W. Li, Semicond. Sci. Technol. **22**, S89 (2007).
6. A.A. Shklyayev and M. Ichikawa, Phys. Rev. B **65**, 045307 (2001).
7. A.A. Shklyayev, M. Shibata, and M. Ichikawa, Phys. Rev. B **62**, 1540 (2000).
8. L. Zhang, H. Ye, Y.R. Huangfu, C. Zhang, and X. Liu, Appl. Surf. Sci. **256**, 768 (2009).
9. V.S. Lysenko, Yu.V. Gomeniuk, Yu.N. Kozyrev, M.Yu. Rubezhanska, V.K. Sklyar, S.V. Kondratenko, Ye.Ye. Melnichuk, and C. Teichert, Adv. Mater. Res. **276**, 179 (2011).
10. Y. Nakamura, M. Ichikawa, K. Watanabe, and Y. Hattugai, Appl. Phys. Lett. **90**, 153104 (2007).
11. Y. Chen, Y.F. Lu, L.J. Tang, Y.H. Wu, B.J. Cho, X.J. Xu, J.R. Dong, and W.D. Song, J. Appl. Phys. **97**, 014913 (2005).
12. J.-M. Baribeau, X. Wu, N.L. Rowell, and D.J. Lockwood, J. Phys. Condens. Matter **18**, R139 (2006).
13. E. Kasper, A. Schuh, G. Bauer, B. Holländer, and H. Kibbel, J. Cryst. Growth **157**, 68 (1995).
14. S.V. Kondratenko, O.V. Vakulenko, Yu.N. Kozyrev, M.Y. Rubezhanska, A.S. Nikolenko, and S.L. Golovinskiy, Nanotechn. **18**, 185401 (2007).
15. V.S. Lysenko, Yu.V. Gomeniuk, V.V. Strelchuk, A.S. Nikolenko, S.V. Kondratenko, Yu.N. Kozyrev, M.Yu. Rubezhanska, and C. Teichert, Phys. Rev. B **84**, 115425 (2011).
16. W. Skorupa, L. Rebohle, and T. Gebel, Appl. Phys. A **76**, 1049 (2003).
17. A.A. Shklyayev and M. Ichikawa, Phys. Uspekhi **51** 133 (2008).
18. A. Barski, M. Derivaz, J.L. Rouvière, and D. Buttard, Appl. Phys. Lett. **77**, 3541 (2000).
19. A.A. Shklyayev, M. Shibata, and M. Ichikawa, Phys. Rev. B **62**, 1540 (2000).
20. Darin Leonhardt, Swapnadip Ghosh, and Sang M. Han, J. Appl. Phys. **110**, 073516 (2011).
21. B.D. Malone, S.G. Louie, and M.L. Cohen, Phys. Rev. B **81**, 115201 (2010).
22. Y. Fujimoto, T. Koretsune, S. Saito, Y. Miyake, and A. Oshiyama, New J. Phys. **10**, 083001 (2008).
23. Y. Kanemitsu, H. Uto, Y. Masumoto, and Y. Maeda, Appl. Phys. Lett. **61**, 2187 (1992).
24. Y. Saito, J. Cryst. Growth **47**, 61 (1979).
25. J. Jiang, K. Chen, X. Huang, Z. Li, and D. Feng, Appl. Phys. Lett. **65**, 1799 (1994).
26. J.C. Jamieson, Science **139**, 762 (1963).
27. A.A. Shklyayev and M. Ichikawa, Appl. Phys. Lett. **80**, 1432 (2002).
28. N.A. Drozdov, A.A. Patrin, and V.D. Tkachev, JETP Lett. **23**, 597 (1976).

Received 02.09.12

## МОРФОЛОГІЯ ТА ОПТИЧНІ ВЛАСТИВОСТІ НАНОКЛАСТЕРІВ Ge НА ОКИСЛЕНІЙ ПОВЕРХНІ Si(001)

*В.С. Лисенко, С.В. Кондратенко, Ю.М. Козирев,  
М.Ю. Рубежанська, В.П. Кладько, Ю.В. Гоменюк,  
О.Й. Гудименко, Є.Є. Мельничук, Ж. Грене, Н.Б. Бланшар*

### Резюме

Розглянуто нанокластери Ge, вирощені методом молекулярно-променевої епітаксії на хімічно окисленій поверхні Si(001) при температурі 700 °C. По дифракції рентгенівських променів

та спектроскопії фотопровідності вперше виявлено, що нанокластери мають кристалічну структуру із об'ємноцентрованою тетрагональною ґраткою, яка має край власного поглинання поблизу 0,48 еВ при 50 К. Нанесення Si на поверхню з нанокластерами Ge приводить до реконструкції поверхні та формуван-

ню полікристалічного покриття із кубічною ґраткою, а об'єм нанокластерів стає твердим розчином SiGe із тетрагональною ґраткою. Край власного поглинання завдяки перемішуванню Si-Ge зазнав зсуву до 0,73 еВ. Обґрунтовано можливий механізм росту нанокластерів.